Supporting Information for

The Synergy of In Situ-generated Ni^0 and Ni_2P to Enhance CO Adsorption and Protonation for Selective CH_4 Production from Photocatalytic CO_2 Reduction

Xuemei Liu, [a#] Chaonan Cui, [b#] Shuoshuo Wei,[a] Jinyu Han, [a] Xinli Zhu, [a] Qingfeng Ge,*[c] Hua Wang*[a]

a Collaborative Innovation Center of Chemical Science and Engineering, Key Laboratory for Green Chemical Technology, School of Chemical Engineering and Technology, Tianjin University, Tianjin, China.
tjuwanghua@tju.edu.cn

b State Key Laboratory for Structural Chemistry of Unstable and Stable Species, Institute of Chemistry, Chinese Academy of Sciences, Beijing 100190, China.

c Department of Chemistry and Biochemistry, Southern Illinois University, Carbondale, IL, 62901, United States
qge@chem.siu.edu

*Corresponding Author: Qingfeng Ge, Hua Wang
E-mail address: qge@chem.siu.edu;
tjuwanghua@tju.edu.cn

EXPERIMENTAL SECTION

1.1 Materials:

Nickel (II) nitrate ($Ni(NO_3)_2 \cdot 6H_2O$, 98%, Aladdin), Triethanolamine ($C_6H_{15}NO_3$, TEOA, 98%, Macklin), Sodium hydroxide (NaOH, 98%, Aladdin), Urea ($CO(NH_2)_2$, AR, Jiangtian Chemical Technology Co., Ltd.), Ammonium oxalate monohydrate ($(NH_4)_2C_2O_4 \cdot H_2O$, AR, Aladdin), Phosphorus red (P, 98.5%, Jiuding Chemical (Shanghai) Technology Co.) were used.

1.2 CO-TPD

CO temperature programmed desorption (TPD) tests were conducted using an automated programmed temperature chemisorption instrument (Chemisorb 2750, Micrometrics). Prior to performing the test, the samples should be pressed and ground, and the samples with a particle size of 40-60 mesh were selected for testing. Test conditions: 100 mg sample was loaded into a U-shaped tube and degassed under argon atmosphere at 300°C for 1 h. After the temperature was reduced to room temperature with gas He, the catalysts were exposed to a stream of CO and He (5% CO) for 1 h to achieve sufficient adsorption of CO, followed by 1 h of He to remove the residual CO. Subsequently, CO desorption of the samples was studied under He atmosphere at a ramp rate of 10°C/min over a temperature range of 30 °C-550 °C.

1.3 Cycle test

Within the three cycle experiments, at the end of a single experiment, the reactor was purged with CO_2 for 3 min, and sealed under dark conditions for 30 min before re-irradiation. To ensure the accuracy of the results, the chromatographic results before re-irradiation were deducted as background.

1.4 In-situ FTIR spectra

In-situ FTIR spectra was obtained with (NICOLET 560, Nicolet). Firstly, 25 mg Ni_2P/CN-0.5 was ground together with 10 mg KBr and pressed. Then the sample was loaded in the reaction chamber and pretreated at 200 °C for 1 h in Ar atmosphere. Next the chamber was cool naturally to room temperature. After that, water vapor saturated CO_2 was supplied to the reaction chamber for 1 h, and then the background spectra was measured. The tracking spectra of the photocatalytic CO_2 reduction were recorded continuously under the illumination of a 300 W Xe lamp.

1.5 Electrochemical characterization

Photoelectric characterization including transient photocurrent response (I-t), electrochemical impedance spectrogram (EIS), and Mott-Schottky (MS) curves were measured using an electrochemical workstation (Auto Lab 302N, Metrohm). A standard three-electrode test system with Pt sheet as the counter electrode, Ag/AgCl electrode as the reference electrode and FTO glass coated with catalyst samples as the working electrode was used for the relevant tests in 0.5 M Na_2SO_4 electrolyte. The preparation of the working electrode: 5 mg of sample was dispersed uniformly in a mixed solution consisting of 245 μL ethanol, 245 μL deionized water and 20 μL Nafion solution by ultrasonication. 20μL of the above suspension was evenly coated on the FTO glass surface (1.0 cm×1.0 cm) with a pipette. Then the electrode was dried at room temperature. The photocurrent curves of the samples were collected using a 300 W Xe lamp coupled to a 420 nm cutoff filter as the light source. The potential measured using Ag/AgCl electrode was converted to NHE scale according to the equation. $E_{NHE} = E_{Ag/AgCl} + 0.197$ V.

1.6 Preparation of Hydro-CN、Ni/CN-0.5 and P/CN-0.5

0.3 g of CN and 0.5 mmol of nickel nitrate were dispersed in 65 mL of H_2O by sonication (1 h) and then stirred for 1 h at room temperature, after which the reaction

was loaded into a 100 mL Teflon autoclave and reacted for 10 h at 140 °C. The product was collected by centrifugation and washed several times with water and ethanol. The samples were dried at 60 °C for 12 h to obtain Ni/CN-0.5; P/CN-0.5 was obtained in a similar way, except that nickel nitrate was replaced by 2.5 mmol red phosphorus. The product Hydro-CN was obtained when the reactant was only CN.

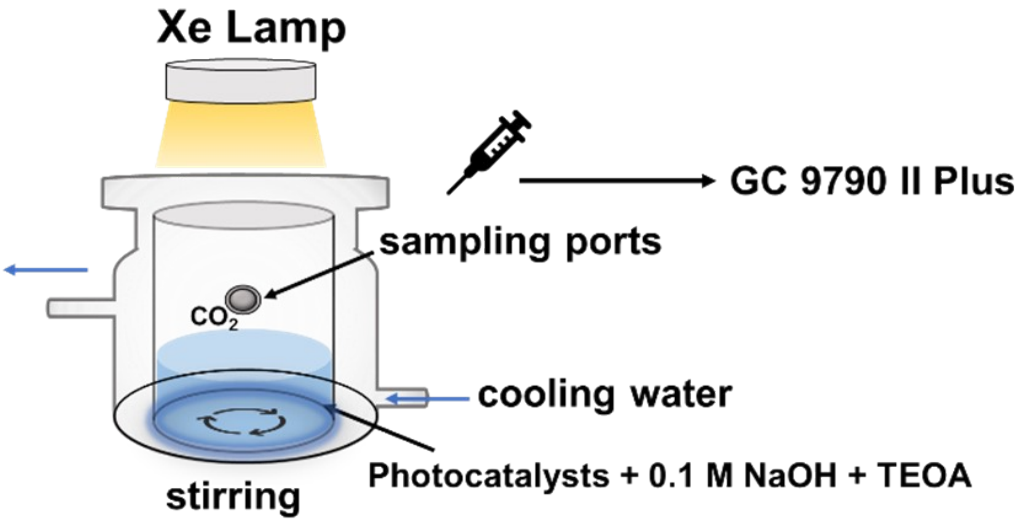

Fig. S1 The schematic diagram of the photocatalytic reaction system.

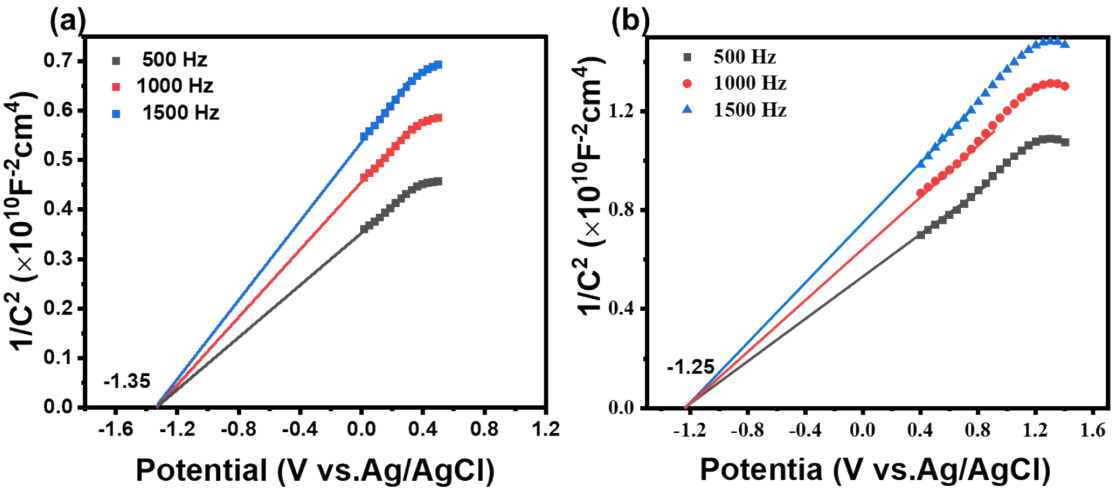

Fig. S2 Mott-Schottky curves of CN and Ni_2P/CN-0.5.

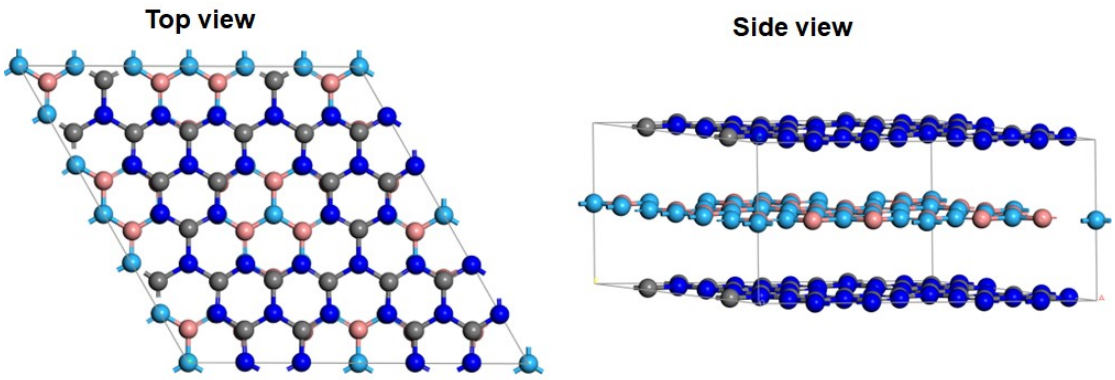

Fig. S3 Optimized structure of bulk g-C_3N_4.

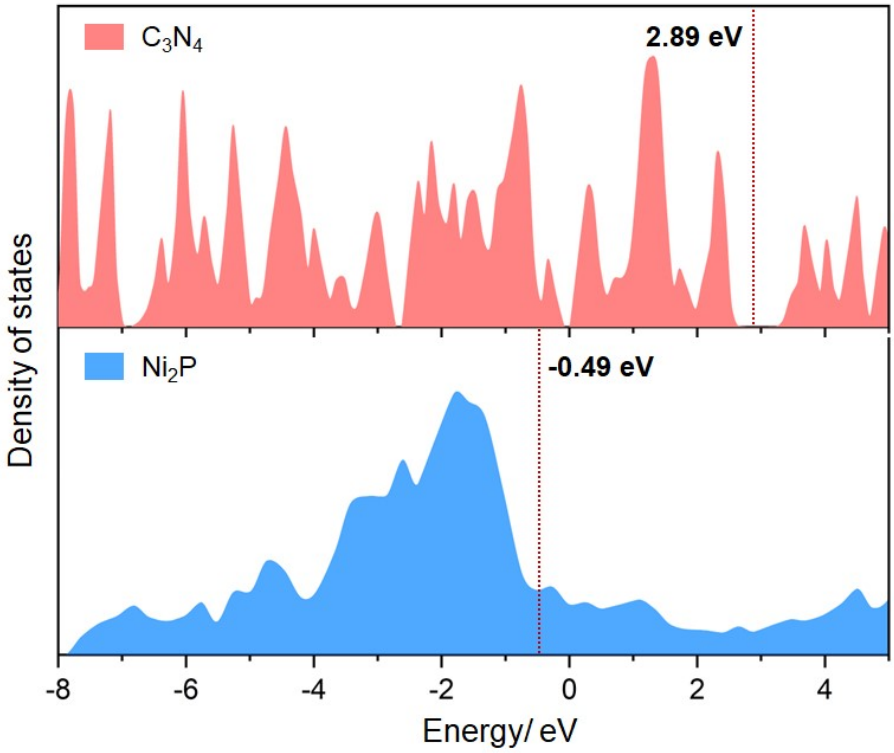

Fig. S4 Density of states and the Fermi level of C_3N_4 and Ni_2P.

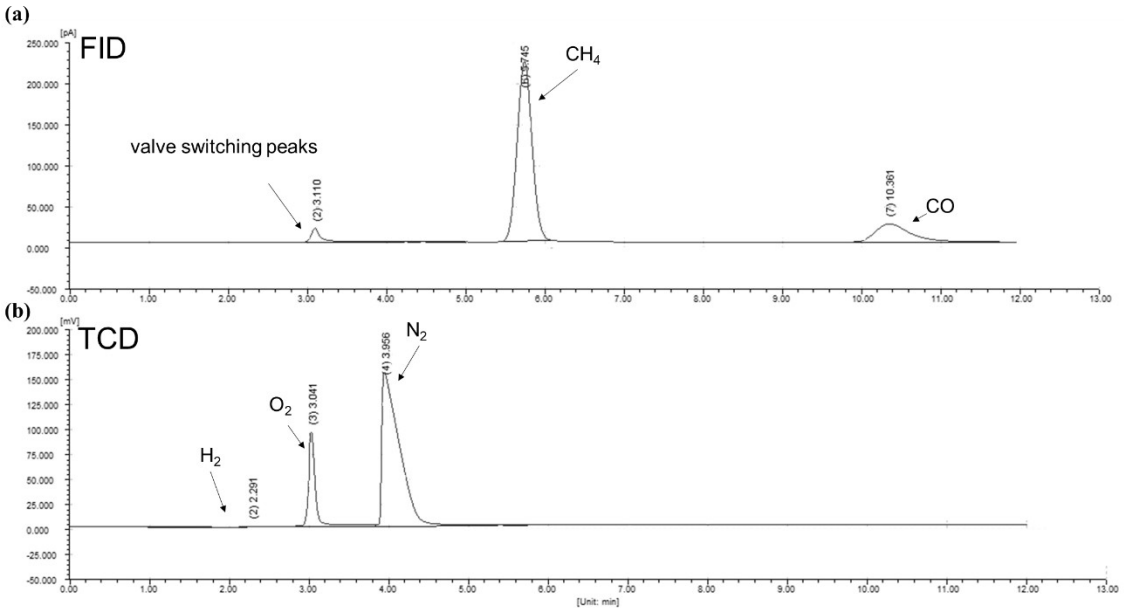

Fig. S5 The GC chromatograms of gas produced during the photocatalytic reduction. (a) FID; (b)TCD.

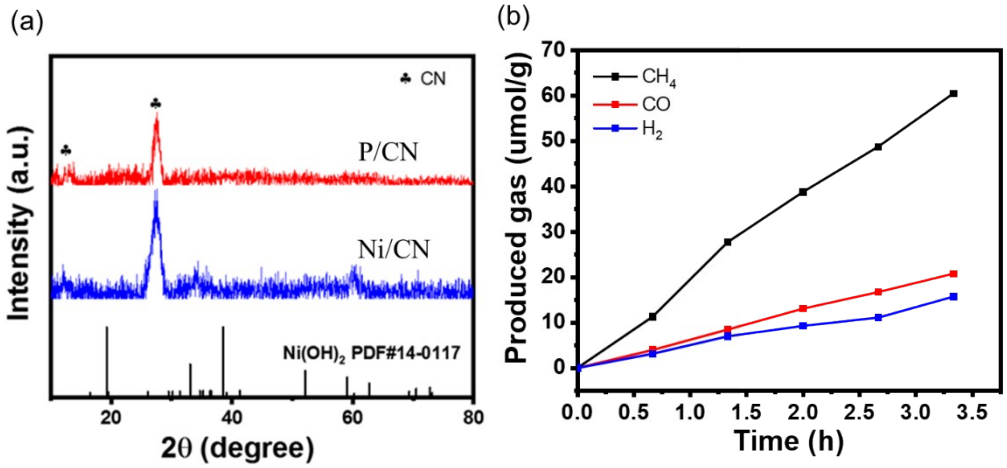

Fig. S6 (a) XRD patterns of P/CN，Ni/CN (b) the product yield profile with reaction time of Ni/CN.

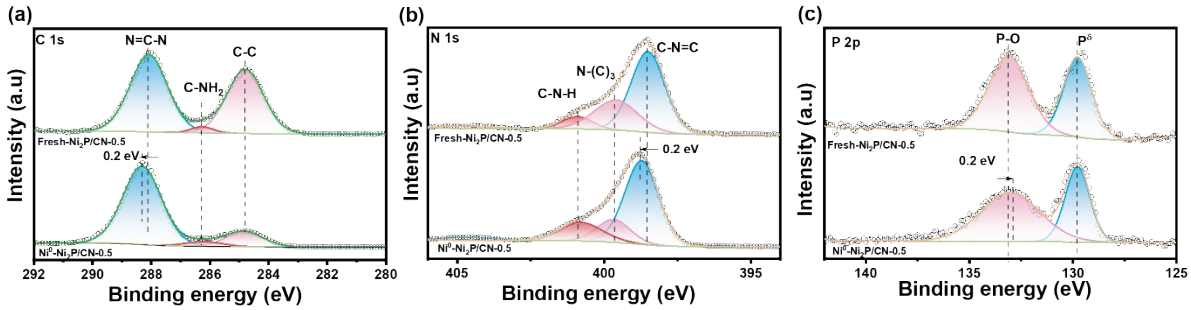

Fig. S7 XPS high-resolution spectra of the fresh Ni_2P/CN-0.5 and Ni^0-Ni_2P/CN-0.5 (a) C 1s, (b) N1s, (c) P 2p.

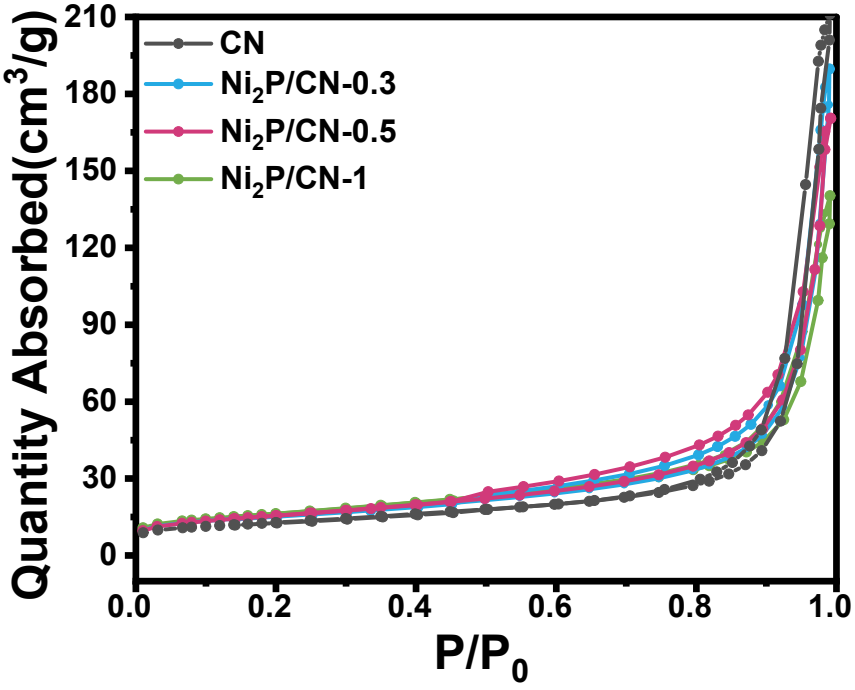

Fig. S8 N_2 adsorption−desorption isotherms of CN and Ni_2P/CN-x.

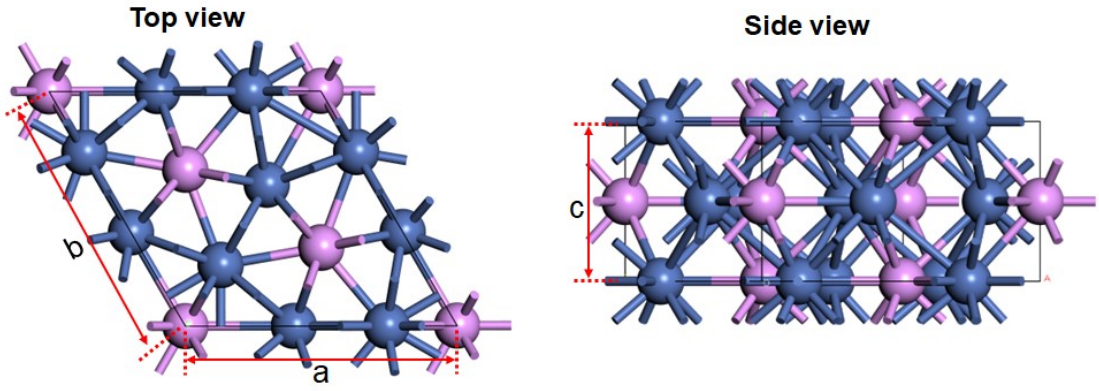

Fig. S9 Unit cell of Ni_2P. The optimized lattice parameters are a=b=5.87 Å, c= 3.36 Å.

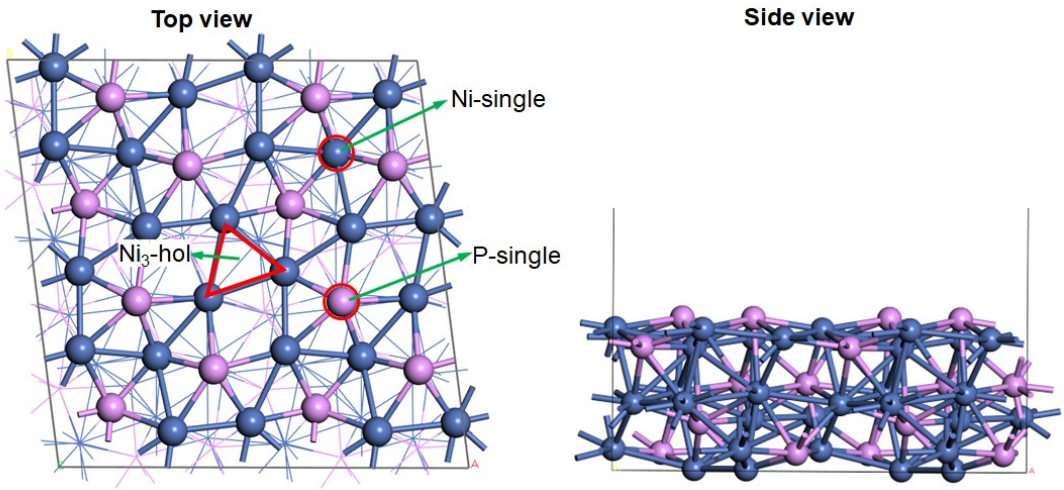

Fig. S10 Optimized structure of Ni_2P (111) surface with three different active sites, i.e., Ni_3-hol, Ni-single and P-single, as labeled in the Fig.

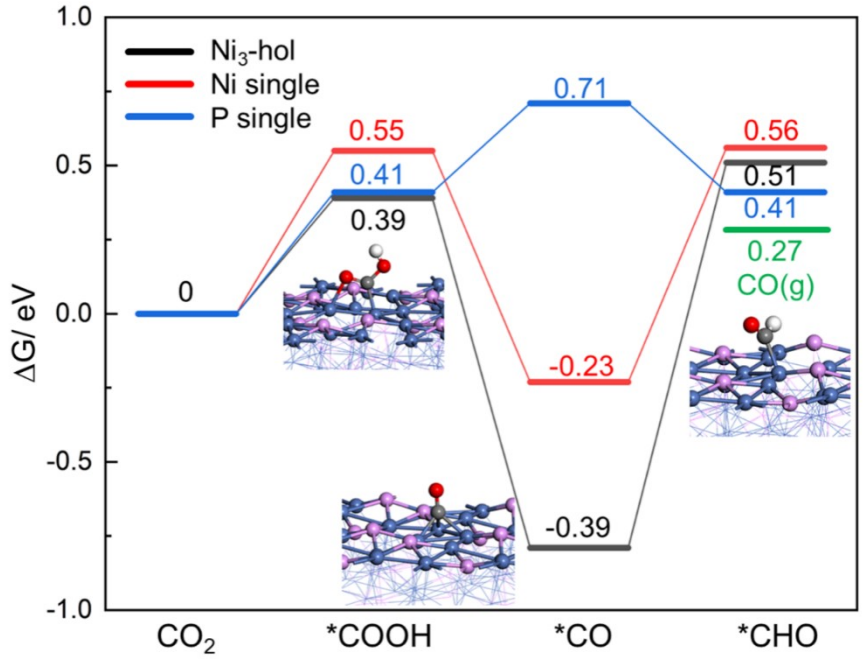

Fig. S11 The Gibbs-free energy (ΔG) profiles for *CHO formation on different active sites of Ni_2P (111).

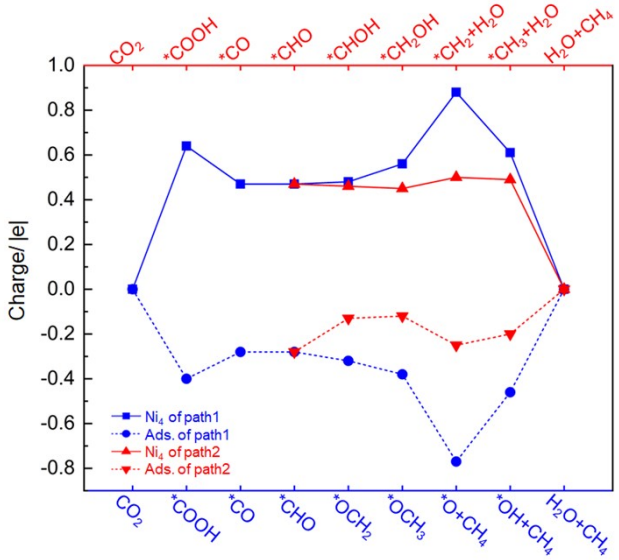

Fig. S12. Bader charge analysis of the intermediates through the path 1 and path 2 on $Ni_4/Ni_2P(111)$.

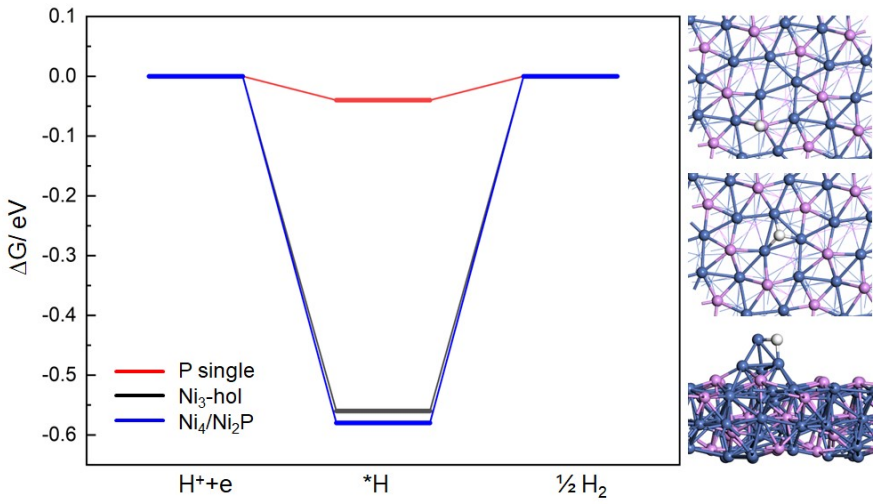

Fig. S13 Energy change for dissociative H^+ into H* and 1/2 H_2 on the different active sites of $Ni_2P(111)$ and (e) Ni_4-cluster of Ni_4/Ni_2P.

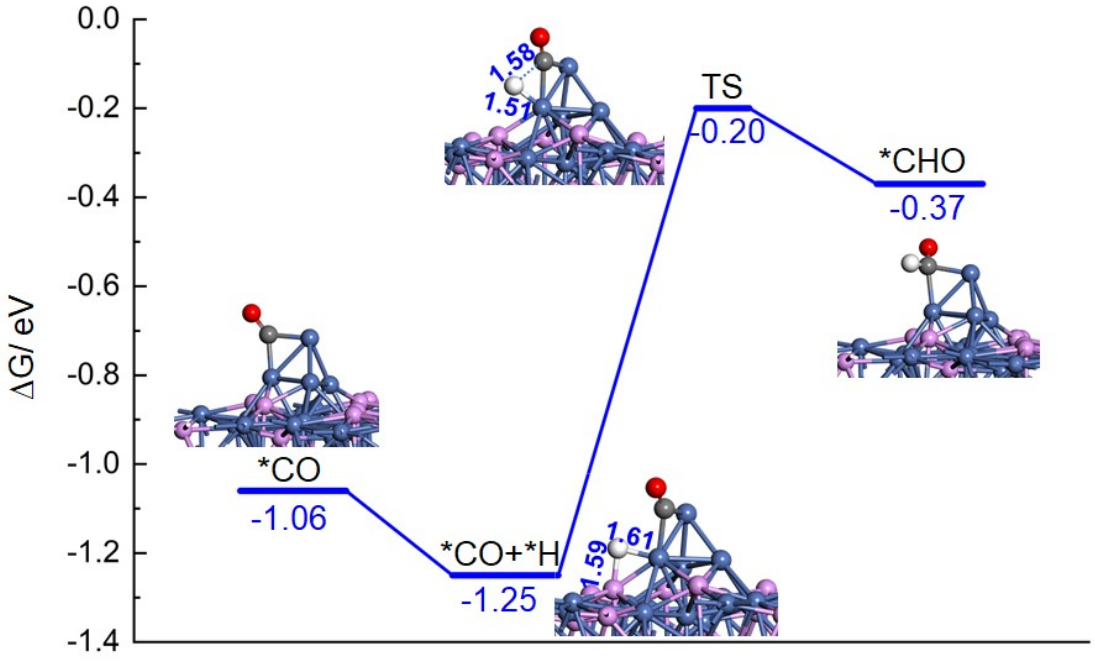

Fig. S14 The Gibbs-free energy (ΔG) change for H transfer from Ni_2P surface to Ni_4 cluster for *CHO formation on Ni_4/Ni_2P (111). The bond length is shown in Å.

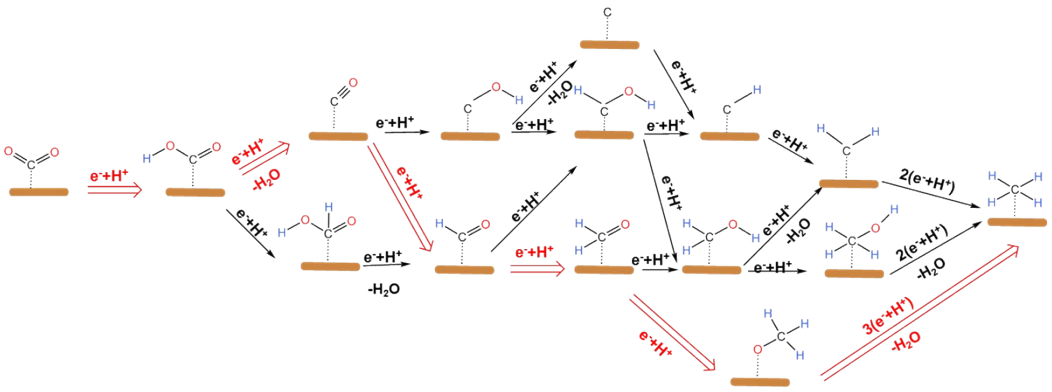

Scheme S1 The possible pathways of photocatalytic CO_2 reduction to CH_4 on the surface of photocatalysts, and the red arrow indicates the formaldehyde mediated reaction pathway.

Table S1 The pH of the reaction system

Reaction solution	pH before the reaction	pH after the reaction
0.1 M NaOH/TEOA	8.2	8.4
H_2O/TEOA	6.5	6.5
0.1M NaOH	8.7	8.7

Table. S2 BET Surface Area, Pore Volume and Pore Diameter Data of CN, Ni_2P/CN-x.

Catalyst	BET surface (m^2/g)	Pore volume （cm^3/g）	Pore size（nm）
CN	57.94	0.15	15.93
Ni_2P/CN-0.3	55.57	0.17	17.70
Ni_2P/CN-0.5	54.83	0.17	17.04
Ni_2P/CN-1	52.42	0.17	17.56

Table S3 The comparison of photocatalytic CO_2 reduction

Photocatalyst	Reaction solvent	Light source	Carbon products	Ref
FeP/CN	H_2O vapor	300 W Xe Lamp	CO 5.19 μmol g^{-1} h^{-1} (5.5 times that of CN)	1
WP-NC/CN	MeCN/H_2O	300 W Xe Lamp	CO 376 μmol g^{-1} h^{-1} (12.9 time that of CN)	2
MoP/CN	H_2O	300 W Xe Lamp	CO 18.3μmol g^{-1} h^{-1} (5.5 times that of CN) CH_4 1.1 (2.0 times that of CN)	3
Cu_3P|S/g-C_3N_4	MeCN/H_2O	300 W Xe Lamp	CO 137 μmol g^{-1} h^{-1} (8.0 times that of CN)	4

$Pd_9Cu_1Hx/g\text{-}C_3N_4$	H_2O vapor	300 W Xe Lamp	CH_4 0.018 μmol h-1 (more than 16 times that of CN)	5
NH_2-MIL-125(Ti)	MeCN/H_2O/TEOA	300 W Xe Lamp	CO 8.25 μmol g^{-1} h^{-1} CH_4 1.01 μmol g^{-1} h^{-1}	6
Ni_2P/CN	NaOH/H_2O/TROA	300 W Xe Lamp	CO 6.81 μmol g^{-1} h^{-1} CH_4 69.02μmol g^{-1} h^{-1} (16.5 times that of CN)	This work

References

1 Y. Guo, Q. Wang, M. Wang, M. Shen, L. Zhang and J. Shi, Catal. Commun., 2021, 156, 106326.

2 X. Zhang, J. Yan, F. Zheng, J. Zhao and L.Y.S. Lee, Appl. Catal. B Environ, 2021, 286, 119879.

3 J. Tang, D. Yang, W. Zhou, R. Guo, W. Pan and C. Huang, J. Catal., 2019, 370, 79-87.

4 X. Zhang, D. Kim, J. Yan and L.Y.S. Lee, Acs Appl. Mater. Inter., 2021, 13, 9762-9770.

5 L. Zhao, F. Ye, D. Wang, X. Cai, C. Meng, H. Xie, J. Zhang and S. Bai, Chemsuschem, 2018, 11, 3524 3533.

6 X. Cheng, X. Dao, S. Wang, J. Zhao and W. Sun, Acs Catal., 2020, 11, 650-658.